PCCP

Accepted Manuscript

ROYAL SOCIETY OF CHEMISTRY

www.rsc.org/pccp

Cite this: DOI: 10.1039/c0xx00000x

www.rsc.org/xxxxxx

ARTICLE TYPE

Dual Function of Living Anionic Polymerization Initiators through the Formation of Chain-End-Protecting Clusters. Support from Density Functional Theory Calculations and Monte Carlo Simulations

Yun Hee Jang,*[a] Yves Lansac,[b] Jae-Ki Kim,[a] Hee-Soo Yoo,[a] Chang-Geun Chae,[a] Cheol Ho Choi,[c] Shashadhar Samal,[a] Jae-Suk Lee*[a]

Received (in XXX, XXX) Xth XXXXXXXXX 20XX, Accepted Xth XXXXXXXXX 20XX

DOI: 10.1039/x0xx00000x

Sodium benzanilide (Na^+BA^-) initiators have opened a new route to a living anionic polymerization of *n*-hexylisocyanate (HIC) with 100% yield and controlled molecular weight. The NaBA initiators do not only provide initiation points for polymerization by attacking HIC monomers but also successfully prevent *back-biting* side reactions without any help from additives. Our hypothesis on this dual function of the NaBA initiators is that they self-assemble to form protection shields around the chain ends. Indeed, our density functional theory calculations in the experimental conditions on the free energy of formation of $(NaBA)_n$ clusters of various sizes and conformations searched by Monte Carlo simulations show that the BA^- moiety forms a stable complex with Na^+ in a fan-like circular-sector shape owing to its double binding sites ($N^-–C=O \leftrightarrow N=C–O^-$) and that the tightly-bound NaBA units spontaneously self-assemble to form small $(NaBA)_n$ clusters (n = 2 and 4). The growing end of the polymer chain $[(BA)(HIC)_n^-]$, which resembles BA^-, would also assemble with n–1 NaBA units to form an n-mer cluster. We expect that the chain end in this cluster would be more available to attack small HIC monomers coming into the cluster (leading to chain growth) rather than folding back to attack the middle of the chain (leading to cyclotrimerization to isocyanurates and depolymerization).

1 Introduction

Polyisocyanate (**1**; Scheme 1), with its helical structure,[1] has been employed in many applications such as optical switches, photonic crystals and chiral recognition.[2-6] It is desirable to have a good control over the molecular weight (MW) and the MW distribution (MWD) of the polymer for these applications. However, initiators commonly used for anionic polymerization of isocyanates, such as metal cyanide,[7] amide,[8,9] alkoxide[10,11] and naphthalenide,[12-16] have not been able to prevent *back-biting* side reactions, in which growing chain ends fold back, attack antepenultimate carbonyl carbons, form cyclic trimers (isocyanurates), and leave from the polymer chains (Scheme 1 of Ref. [17]).[7] Additives such as crown ether and sodium tetraphenylborate[12-16] increase control over MW and MWD by supressing the back biting.

Sodium benzanilide (Na^+BA^-) initiators (Scheme 1), on the other hand, enables living anionic polymerization of *n*-hexyl isocyanate (HIC; $C_6H_{13}N=C=O$) with 97–100% yield, controlled MW, narrow MWD (1.08–1.16 of polydispersity index) without any help from additives.[18-20] This initiator does not only provide initiation points for polymerization by attacking HIC monomers but also successfully prevents the back biting. The origin of the dual function served by the NaBA initiator is not fully understood. On the basis of the low initiation efficiency (20±1%) and the long reaction time (60–70 min) observed for its HIC polymerization,[18] we formulate a hypothesis that the Na^+ and BA^- units aggregate around the chain ends to form a protection shield against the back biting. Initiators such as lithium amide and alkoxide aggregate as well,[21-23] but what is particular with NaBA is that BA^- has a double-nucleophile amidate end ($N^-–C=O \leftrightarrow N=C–O^-$) which resembles the growing end of the poly-HIC chain ($BA–HIC^-$; Scheme 1). Spontaneous formation of $(NaBA)_n$ clusters would lead to spontaneous formation of $(NaBA–HIC)(NaBA)_{n-1}$ clusters (Scheme 2 for an example of n = 4). The $BA–HIC^-$ chain end surrounded by n–1 NaBA units in the bulky n-mer cluster would have difficulty in attacking the antepenultimate carbonyl sites.

SCHEME 1

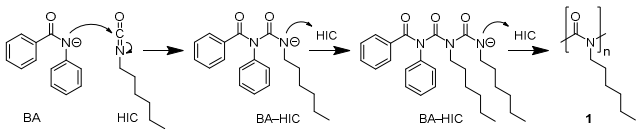

SCHEME 2

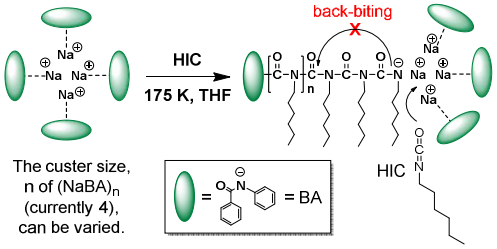

Proving the presence of $(NaBA)_n$ clusters would be the first step to confirming our hypothesis. Since it is difficult to detect them from experiments, we instead use density functional theory (DFT) to estimate the relative stabilities of $(NaBA)_n$ clusters of various sizes (n) in the polymerization conditions, that is, the tetrahydrofuran (THF) solution at −98°C (175 K).

2 Calculation Details

The stability of each $(NaBA)_n$ cluster in THF at 175 K is given by the free energy of self-assembly ($\Delta\Delta G^0_{SA}$), which is defined as the change in the standard Gibbs free energy during the self-assembly of n units of NaBA (Table S1):

$$\Delta\Delta G^0_{SA} = \Delta G^0_{THF}[(NaBA)_n] - n \times \Delta G^0_{THF}(NaBA) . \quad (1)$$

The standard Gibbs free energy of each species in THF at 175 K (ΔG^0_{THF}) is the sum of the gas-phase standard free energy at 175 K (ΔG^0_g) and the standard free energy of solvation in THF (ΔG^0_{solv}). The gas-phase standard free energy at 175 K (ΔG^0_g) is the sum of the gas-phase energy at 0 K (ΔE_0), the zero-point energy (ZPE) and the Gibbs free energy change from 0 to 175 K ($\Delta\Delta G_{0\to175K}$):

$$\Delta G^0_{THF} = \Delta G^0_g + \Delta G^0_{solv} = \Delta E_0 + (ZPE) + \Delta\Delta G_{0\to175K} + \Delta G^0_{solv} . \quad (2)$$

We obtain ΔE_0 (Table S1) from a full geometry optimization of each species at the B3LYP/6-311G(d,p) level of DFT[24-28] with the *Jaguar* v6.5 software.[29,30] A variety of initial structures of free BA^-, free NaBA complex, and $(NaBA)_n$ clusters are prepared for the geometry optimization. Initial structures for clusters with high symmetries (linear Na configuration for n = 2; triangular for n = 3; square and tetrahedral for n = 4; pentagonal for n = 5; hexagonal and octahedral for n = 6) are constructed on the basis of crystallographic[31-34] and computational[22,23,32-35] studies on similar aggregates. A Metropolis MC conformation search[36] with the OPLS-AA force field[37,38] implemented in the *MacroModel* v9.1 software[39] generates other initial structures for each cluster size by varying the dihedral angles in BA^- as well as the relative positions and orientations between Na^+ and BA^- units. The five most stable distinctive structures of each MC search are submitted to the DFT geometry optimization.

The ZPE and $\Delta\Delta G_{0\to175K}$ values should be estimated from the translational, rotational, and vibrational energy levels of each species. However, for a cluster held with soft non-covalent bonds, a normal mode analysis of the vibrational energy levels within a harmonic approximation is difficult and most likely unreliable.[23] Since the major change in molecular motions during aggregation is in translations and rotations rather than in vibrations,[23,32,40-42] we skip the time-consuming normal mode analysis and the evaluation of the supposedly negligible[41] ZPE and vibrational contribution to $\Delta\Delta G_{0\to175K}$. Only the translational and rotational contributions to $\Delta\Delta G_{0\to175K}$ are estimated from the equipartition theorem and the ideal gas approximation (Table S1).[43] The validity of this approach is confirmed for the small species, BA^- and $(NaBA)_n$ (n = 1–2). [The relative ΔG^0_{THF} values shown in Fig. 1 and the $\Delta\Delta G^0_{SA}$ values shown in Fig. 2 are within ~1 kcal/mol from those including the ZPE and the full vibration contributions evaluated from the normal mode analyses: **0a** (6.9), **1b** (2.3), **1c** (2.7), **1d** (7.3); **2a** (–2.7), **2b** (2.3), **2c** (8.5), and **2d** (8.7).]

We calculate ΔG^0_{solv} (Table S1) with a continuum-solvation model by solving a Poisson-Boltzmann equation combined with DFT,[44,45] which has been successfully used[46-49] as an alternative to explicit-solvent models. A solute molecule is described as a low-dielectric cavity (ε_{solute} = 1)[44,45] immersed in a high-dielectric continuum (ε_{THF} = 7.52)[50] representing the THF solvent. The solute–solvent boundary is described by the surface of the closest approach as a sphere of radius 2.53 Å (the probe radius[29] of THF estimated from its density 0.8833 g/cm^3 and MW 72.106)[50] is rolled over the van der Waals envelope of the solute.[44,45] The atomic radii used to build the solute envelope are (in Å): 1.15 (H), 1.9 (C), 1.6 (N and O) and 1.491 (Na).[29] The solution-phase calculations are carried out at the B3LYP/6-311G(d,p) level of DFT as in the gas-phase calculation. The solute geometry is re-optimized in solution. The Cartesian coordinates of the optimized geometries are listed in Table S2. Due to a decrease in the solute–solvent contact area, aggregation of n NaBA units into an $(NaBA)_n$ cluster would experience a significant amount of desolvation penalty, that is, a significant increase in the free energy of solvation due to aggregation, $\Delta\Delta G_{solv}$ = ΔG^0_{solv} $[(NaBA)_n] - n \times \Delta G^0_{solv}(NaBA)$. This penalty, which is evaluated as 35.0, 67.8, 99.7, 114.4 and 165.7 kcal/mol for **2a**–**6a** (n = 2–6 in Figs. 2–6 below), results in a lower degree of aggregation n in the THF solution than in the gas phase.

For a seamless combination with ΔG^0_g to give ΔG^0_{THF} in Eq. 2, ΔG^0_{solv} should represent the free energy change for the standard solvation process corresponding to a transfer of a solute from the gas-phase standard state (ideal gas at 1 atm) into the solution-phase standard state (1 M ideal solution). However, most solvation free energy calculations including ours have been developed on the basis of experimental solvation free energies corresponding to a transfer of a solute from 1 M gas phase into 1 M solution phase. Hence we need to add a free energy correction which represent the work to bring 1 mol of gas from 1 atm (22.47 L/mol) to 1 M (1 mol/L), that is, the free energy of compression from 22.47 L to 1 L [$\Delta G_{1atm\to1M} = \Delta G_{22.47L\to1L} = RT \ln (22.47/1)$ = 1.08 kcal/mol]. This essentially corresponds to a correction for the reduction of molecular free volume during a transfer from gas to solution,[40] and adds a constant correction (1.08 kcal/mol) to ΔG^0_{solv} for all species (Table S1). This leads to a decrease in the desolvation penalty by 1.08 × (n − 1) kcal/mol, making the formation of large $(NaBA)_n$ clusters more favourable.

Similarly, the Sackur-Tetrode (ST) equation[43] used to estimate the translational entropy as a part of $\Delta\Delta G_{0\to175K}$ in Eq. 2 would be inappropriate to estimate the translational entropy of a solute in 1 M solution (with a tendency of overestimation).[40] The assumption that solutes have no volume is reasonable in the gas phase, since the volume occupied by the solutes is much smaller than the total volume so that the solutes can move around freely in it. On the other hand, most of the total volume in condensed phases is occupied by the solvent, so that a greatly reduced amount of free volume would remain for the solutes.[40,41] We thus evaluate the translational entropy (Table S1) of the solute in the remaining free volume (in cal mol^{-1} K^{-1}) using the following equations,[40]

$$S^{solute}_{trans} = 2.65 + 2.99 \ln T + 2.99 \ln M + [\Delta S^{solvent}_{cond,exp} - \Delta S^{solvent}_{cond,ST}] , \quad (3)$$

where

$$\Delta S^{solvent}_{cond,ST} = S^{THF}_{l,ST} - S^{THF}_{g,ST} = 1.99(\ln[THF]_l - \ln[THF]_g) = -11.16 . \quad (4)$$

The experimental entropy of condensation of THF ($\Delta S^{solvent}_{cond,exp}$ =

$S^{THF}_{l,exp} - S^{THF}_{g,exp}$ = 48.83 – 72.58 = –23.45 cal mol^{-1} K^{-1}),[50] the mass M of $(NaBA)_n$ cluster (n × 219.219 g/mol) and the temperature T (175 K) are plugged into Eq. 3. The concentrations of THF in the standard-state gas phase (0.0446 M for 1 mol per 22.4 L) and liquid phase (12.25 M for a density of 0.8833 g/cm^3 and an MW of 72.106 g/mol)[50] are plugged into Eq. 4.

3 Results and Discussion

Fig. 1 shows the geometry-optimized major conformers of free BA^- and NaBA. For free BA^- **0**, the *cis* conformer **0a** is *less* stable than the *trans* conformer **0b** by 7.4 kcal/mol. The steric hindrance between two phenyl rings of **0a** significantly twists the dihedral angles ∠CNC(=O)C, ∠CCNC(=O) and ∠NC(=O)CC by ~30°, while **0b** is completely planar. On the other hand, in the case of the NaBA unit complex **1**, the *cis* conformer **1a** is more stable than the *trans* conformers **1b–1d** by 2.8–7.3 kcal/mol despite the twist. This should be because BA^- in **1a** makes a bidentate bonding to Na^+ through both $O^{\delta-}$ and $N^{\delta-}$ (N^-–C=O ↔ N=C–O^-) [r(Na···O) = 2.34 Å; r(Na···N) = 2.46 Å], while only one of them ($O^{\delta-}$ or $N^{\delta-}$) is used to bind Na^+ in **1b–1d** [r(Na···O) = 2.22 Å (**1b**), 2.20 Å (**1c**); r(Na···N) = 2.38 Å (**1d**)]. The binding free energy of **1a**, which is defined as

$$\Delta\Delta G_{bind} = \Delta G_{THF}(NaBA) - \Delta G_{THF}(Na^+) - \Delta G_{THF}(BA^-), \qquad (5)$$

is –15.3 kcal/mol. Such negative value indicates that the NaBA unit complex, **1a** in particular, can form spontaneously and stay strongly bound in THF at 175 K. With its fan-like circular-sector shape, the **1a** unit is expected to self-assemble further.

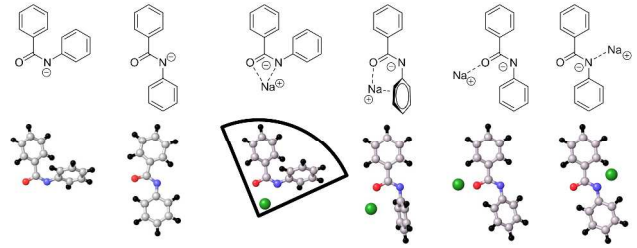

Fig. 1 Major conformers of free BA^- (**0a**–**0b**) and unit complex NaBA (**1a**–**1d**). Relative free energies (kcal/mol) between species of the same size are shown in parentheses. The most stable species is marked with underline. [Color code: Na (green), O (red), N (blue), C (grey), H (black)]

Fig. 2 shows the optimized geometries of major conformers of $(NaBA)_2$ cluster **2**. The pseudo-two-dimensional (nearly planar) *cis* conformer with C_i symmetry (**2a**) is the most stable among them. It is 11 kcal/mol more stable than the *trans* conformers **2c**–**2d**. In this *cis* conformer **2a** (and similarly in **2b**) each Na^+ is triply coordinated (to $O^{\delta-}$ and $N^{\delta-}$ from one BA^- at 2.25 and 2.46 Å and to $O^{\delta-}$ from the other BA^- at 2.43 Å), while each Na^+ in the minor *trans* conformers **2c–2d** is only doubly coordinated (to $O^{\delta-}$ from one BA^- at 2.23 Å and to $N^{\delta-}$ from the other BA^- at 2.42 Å). The Na^+···Na^+ distance is shorter in **2a–2b** (3.27 and 3.11 Å) than in **2c–2d** (4.96 and 4.73 Å). The predominant conformer **2a** exhibits a slightly negative free energy of self-assembly (–1.7 kcal/mol) with respect to a separate pair of the predominant **1a** units. This **2a** cluster would form spontaneously but would stay loosely bound. The $N^{\delta-}$ site binds less strongly to Na^+ than the $O^{\delta-}$ site in **2a** and especially in slightly less stable **2b**. This site would still be able to attack HIC monomers for the chain growth.

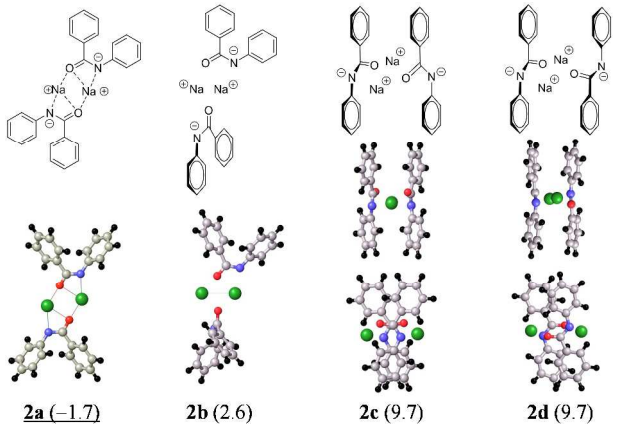

Fig. 2 Major conformers of $(NaBA)_2$ complexes **2a**–**2d**. Two side views are shown for **2c**–**2d**. In parentheses are shown the free energies of self-assembly (kcal/mol) relative to a separate pair of the most stable NaBA units (**1a**). The most stable species is marked with an underline.

Fig. 3 shows the optimized geometries of major conformers of $(NaBA)_3$ cluster **3**. The situation is similar to the $(NaBA)_2$ cluster. A pseudo-two-dimensional *cis* conformer **3a** with a necklace-like shape is the most stable. Each Na^+ in **3a** is triply coordinated to $O^{\delta-}$ and $N^{\delta-}$ at 2.3–2.5 Å and the Na^+···Na^+ distance is ~4.0 Å, while each Na^+ in the less stable *trans* conformer **3c** is only doubly coordinated to $O^{\delta-}$ and $N^{\delta-}$ at 2.2–2.4 Å and the Na^+···Na^+ distance is ~5.6 Å. However, the positive value of the free energy of self-assembly indicates that the NaBA units are unlikely to self-assemble to this size of clusters. The trend exhibited by the clusters **1**–**3** that the *cis* conformers are preferred to the *trans* conformers is expected to continue for larger $(NaBA)_n$ clusters. Hence only the *cis* conformers are considered for $(NaBA)_n$ clusters with $n \geq 4$.

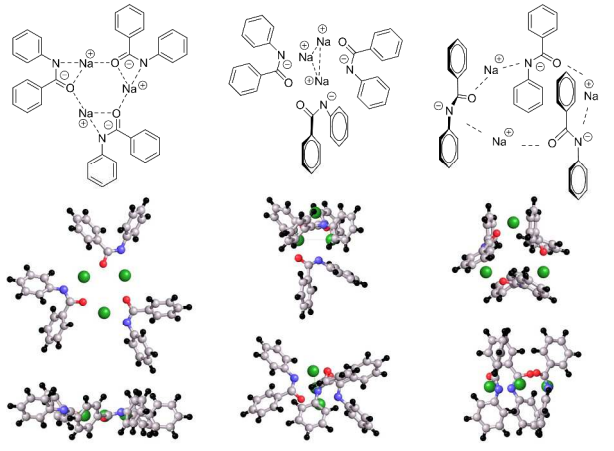

Fig. 3 Top and side views on the major conformers of $(NaBA)_3$ cluster (**3a**–**3c**) and their free energies of self-assembly (kcal/mol) relative to a separate triplet of the most stable NaBA units **1a**. The most stable species (pseudo-two-dimensional *cis* conformer **3a** with a necklace-like shape) is marked with an underline.

Fig. 4 shows the optimized geometries of major *cis* conformers of $(NaBA)_4$ clusters. A three-dimensional cube-type prismane conformer **4a**, which is made of two **2a** units put together, is the most stable form of $(NaBA)_4$. Each Na^+ in the **4a** conformer is coordinated to four binding sites (one $N^{\delta-}$ and three $O^{\delta-}$ sites). It is 8 kcal/mol more stable than the pseudo-two-dimensional necklace-type conformer **4c**, in which each Na^+ is coordinated to three binding sites only (one $N^{\delta-}$ and two $O^{\delta-}$ sites). The free energy of self-assembly to **4a** is slightly negative (–1.5 kcal/mol) with respect to a well-separated quartet of the most stable NaBA units (**1a**). This indicates that NaBA units would spontaneously self-assemble to form loosely-bound **4a** clusters.

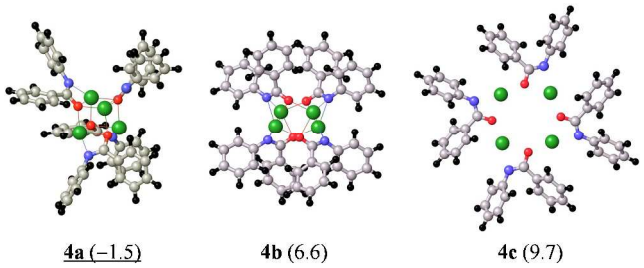

Fig. 4 Major *cis* conformers **4a**–**4c** of $(NaBA)_4$ and their free energies of self-assembly (kcal/mol) relative to four well-separated **1a** units. The most stable species (three-dimensional cube-type **4a** rather than pseudo-two-dimensional necklace-type **4c**) is marked with an underline.

Fig. 5 shows the optimized geometries of major *cis* conformers of $(NaBA)_5$ and $(NaBA)_6$ clusters **5**–**6**. Among $(NaBA)_5$ clusters, the pseudo-two-dimensional necklace-type conformer **5a** is the most stable. On the other hand, among $(NaBA)_6$ clusters, a three-dimensional hexaprismane conformer **6a**, which is made of three **2a** units put together, is the most stable (18 kcal/mol more stable than the peudo-two-dimensional necklace-type conformer **6b**). The positive values of the free energy of self-assembly (15.8 and 3.0 kcal/mol for **5a**–**6a**) indicate that the NaBA units are unlikely to self-assemble to these sizes of clusters (and to larger clusters).

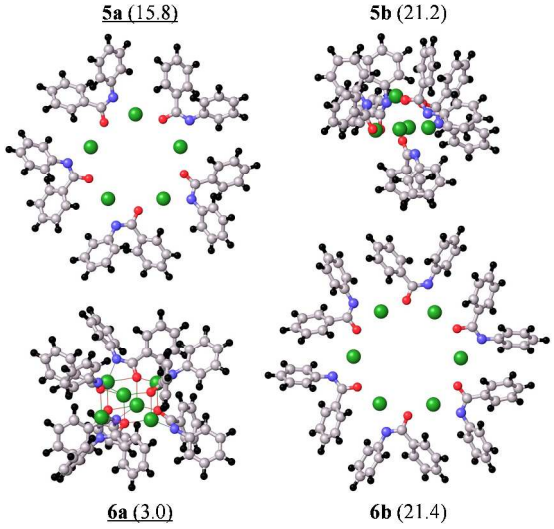

Fig. 5 Major *cis* conformers **5a**–**5b** of $(NaBA)_5$ and **6a**–**6b** of $(NaBA)_6$ and their free energies of self-assembly (kcal/mol) relative to the same number of separate **1a** units. The most stable species (pseudo-two-dimensional necklace-type **5a** and three-dimensional hexaprismane **6a**) are marked with an underline.

Now that the most stable conformers among the considered ones are identified for the $(NaBA)_n$ clusters (**1a**–**6a** for n = 1–6), their free energies of self-assembly with respect to n separate **1a** units ($\Delta\Delta G_{SA}$) are plotted together in Fig. 6: –1.7 (**2a**), 3.7 (**3a**), –1.5 (**4a**), 15.8 (**5a**) and 3.0 (**6a**) kcal/mol. The most favorable NaBA species in THF at 175 K (positioned in the green area of Fig. 6) are the smallest pseudo-two-dimensional cluster **2a** made of two **1a** units put together ($\Delta\Delta G_{SA}$ = –1.66 kcal/mol) as well as the smallest three-dimensional cluster **4a** made of two **2a** units put together ($\Delta\Delta G_{SA}$ = –1.54 kcal/mol). With a very small energy difference of 0.12 kcal/mol, the **2a** and **4a** clusters would be in dynamic equilibrium with each other, and they would be in equilibrium with a small portion of the tightly-bound NaBA unit **1a** ($\Delta\Delta G_{bind}$ = –15.3 kcal/mol). A presence of $(NaBA)_n$ clusters (n = 2 and 4) in equilibrium with a contact-ion NaBA unit is hence shown to be plausible, supporting our hypothesis on the dual function of the NaBA initiators. The aggregation degree of 2 to 4 has also been well known for lithium-based initiators in THF.[22,35]

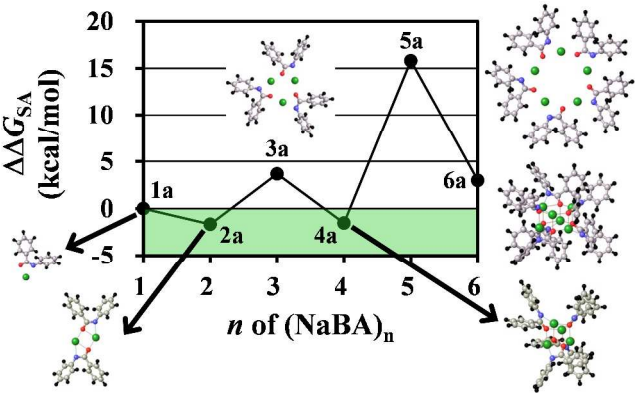

Fig. 6 Free energy of self-assembly to the most stable conformation of each size of $(NaBA)_n$ clusters (**2a**–**6a**) with respective to n well-separated **1a** NaBA units. Clusters with lower $\Delta\Delta G_{SA}$ values are more favorable and those with negative $\Delta\Delta G_{SA}$ (in the green area) would form spontaneously.

The growing end of the polymer chain (BA–HIC^-) also makes a strong bond with Na^+ ($\Delta\Delta G_{bind}$ = –19.4 kcal/mol) to form the same type of complex (not shown here) as the fan-shape NaBA unit **1a**. Therefore, if the formation of $(NaBA)_2$ and $(NaBA)_4$ clusters is spontaneous formation, the integration of the growing chain end in (NaBA–HIC)(NaBA) and (NaBA–HIC)$(NaBA)_3$ clusters would also be spontaneous (see Scheme 2 for the latter case of n = 4). The growing chain ends hidden in these clusters would not be available for the back-biting attacks to the antepenultimate sites of the polymer chains which are stiff (due to the amide backbone) and hairy (due to the *n*-hexyl side chains). Hence the depolymerisation through the formation of cyclic trimers would be avoided, as shown in Scheme 1 of Ref. [17]. On the other hand, an HIC monomer with its slender linear shape would still come into these clusters due to the electrostatic attraction between Na^+ and $O^{\delta-}$=$C^{\delta+}$=NC_6H_{13}, as shown in Scheme 2. The HIC monomer would prefer being near the growing chain end due to the van der Waals interaction between the *n*-hexyl side chains. The carbonyl ($O^{\delta-}$=$C^{\delta+}$) bond of the incoming HIC would be even more polarized by its interaction with Na^+, being more ready for a nucleophilic attack either by the grown chain end BA–HIC^- or by the initiator BA^-. We expect

that the HIC would be preferentially attacked by the growing chain end rather than by the initiator because the aliphatic N^- of $BA–HIC^-$ has a higher basicity (and in turn a higher nucleophilic reactivity towards the electrophilic carbonyl carbon of HIC) than the aromatic N^- of BA^-. Therefore, the predominant process occurring in these clusters would be a continuous growth of the existing $BA–HIC^-$ chain rather than a back-biting attack to the antepenultimate carbonyl group by the $BA–HIC^-$ chain end or an initiation of a new chain by a BA^- initiator. This process would successfully lead to a living anionic polymerization of HIC with no need of additives. This is similar to the bifunctional activation mechanism (insertion, polarization and addition) proposed for the living coordination polymerization of HIC[51] and the fixation of isoelectronic carbon dioxide[52] by organotitanium(VI) catalysts. A considerably lower reactivity of aggregated initiators than non-aggregated contact ion pairs explains the low initiation efficiency (20±1%) and the long reaction time (60–70 min) observed for the HIC polymerization by the NaBA initiator.[18] One concern is that, if the two different sizes of active species, $(NaBA)_2$ and $(NaBA)_4$, have different reactivities towards HIC (which can be checked with DFT calculations), their presence in equilibrium would lead to a poor control of MWD and this is not consistent with the observed MWD of 1.08–1.16.[18]

It is also possible that the true active species in the initiation could be the non-associated NaBA unit, which would be present in a low concentration in equilibrium with more stable $(NaBA)_2$ and $(NaBA)_4$ aggregates which would play a role of dormant species protecting the activated chain end from the back-biting.[22] This mechanism is consistent not only with the experimentally-observed low initiation efficiency and long reaction time but also with the good control of MWD (1.08–1.16) by NaBA.[18]

Such issue, that is, the size n of $(NaBA)_n$ clusters participating in the initiation, can be estimated from a relationship ($\log k^{app}$ = constant + $1/n$ $\log$ [NaBA])[53,54] between the concentration of NaBA ([NaBA]) and the apparent reaction constant (k^{app}) estimated from absorbance measurements.[53,54] However, the overlap between the absorption spectra of NaBA and PHIC as well as the low reaction temperature (175 K) may hamper such measurements. In this case, DFT calculations will be carried out on the detailed reaction mechanism of the HIC polymerization by NaBA as the last resort as well as on the possibility of using this process for carbon dioxide capture and conversion will be reported separately. This information would be further combined with a continuum (or off-lattice) kinetic MC method to simulate the self-assembly of NaBA, the initiation of HIC (or carbon dioxide) by NaBA and the growth into poly-HIC (or polycarbonate), as recently done for an investigation of the initial stage of polymerization of silicates from water solution.[55,56]

4 Conclusions

Our DFT calculations on NaBA initiators combined with MC conformation search, Poisson-Boltzmann continuum-solvation approach, Gibbs free energy correction at 175 K and free volume correction for THF confirms that tightly-bound contact-ion NaBA units (**1a**) would spontaneously self-assemble into loosely-bound $(NaBA)_2$ and $(NaBA)_4$ aggregates (**2a** and **4a**). It constitutes the first step to support our hypothesis on the origin of the successful living anionic polymerization of HIC by NaBA without any help from additives. Our hypothesis on the reaction mechanism of the HIC polymerization controlled by the NaBA clusters will be confirmed in a separate report.

Acknowledgments

This work was supported by the Korean CCS 2020 Program (2013M1A8A1040838), the Global Frontier Hybrid Interface Materials Program (2013M3A6B1078882), the Basic Research Program (2013R1A1A3012254) and the Korea-India SAVI Program (2013K2A1B9066145) funded by the Ministry of Science, ICT & Future Planning. This work was also supported by the Brain Pool Program (121S-1-3-0380 and 131S-1-3-0504) of KOFST, the Inter-ER Cooperation Project (R0000499) of KIAT/MKE, the Grand Challenge Program (KSC-2013-C3-026) and the PLSI supercomputing resources of KISTI, and also by GIST Specialized Research Project of GIST.

Notes and references

[a] Gwangju Institute of Science and Technology, Gwangju, Korea.
[b] GREMAN, Université François Rabelais, Tours, France.
[c] Kyungpook National University, Daegu, Korea.

† Electronic Supplementary Information (ESI) available: the free energy components and the Cartesian coordinates for the DFT optimized structures of **0a**–**6b**. See DOI: 10.1039/b000000x.

1. A. J. Bur and L. J. Fetters, *Chem. Rev.*, 1976, **76**, 727-746.
2. D. Pijper, M. G. M. Jongejan, A. Meetsma and B. L. Feringa, *J. Am. Chem. Soc.*, 2008, **130**, 4541-4552.
3. J.-H. Kim, M. S. Rahman, J.-S. Lee and J.-W. Park, *J. Am. Chem. Soc.*, 2007, **129**, 7756-7757.
4. G. M. Miyake, R. A. Weitekamp, V. A. Piunova and R. H. Grubbs, *J. Am. Chem. Soc.*, 2012, **134**, 14249-14254.
5. M. Changez, N.-G. Kang, H.-D. Koh and J.-S. Lee, *Langmuir*, 2010, **26**, 9981-9985.
6. E. Yashima, K. Maeda, H. Iida, Y. Furusho and K. Nagai, *Chem. Rev.*, 2009, **109**, 6102-6211.
7. V. E. Shashoua, *J. Am. Chem. Soc.*, 1959, **81**, 3156-3156.
8. Y. Okamoto, M. Matsuda, T. Nakano and E. Yashima, *J. Polymer Sci., Part A: Polym. Chem.*, 1994, **32**, 309-315.
9. K. Maeda and Y. Okamoto, *Macromolecules*, 1999, **32**, 974-980.
10. N. Fukuwatari, H. Sugimoto and S. Inoue, *Macromol. Rapid Commun.*, 1996, **17**, 1-7.
11. T. Ikeda, H. Sugimoto and S. Inoue, *J. Macromol. Sci. Part A: Pure Appl. Chem.*, 1997, **34**, 1907-1920.
12. J.-S. Lee and S.-W. Ryu, *Macromolecules*, 1999, **32**, 2085-2087.
13. Y.-D. Shin, J.-H. Ahn and J.-S. Lee, *Polymer*, 2001, **42**, 7979-7985.
14. Y.-D. Shin, S.-Y. Kim, J.-H. Ahn and J.-S. Lee, *Macromolecules*, 2001, **34**, 5071-5071.
15. J.-H. Ahn and J.-S. Lee, *Macromol. Rapid Commun.*, 2003, **24**, 571-575.
16. J.-H. Ahn, C.-H. Lee, Y.-D. Shin and J.-S. Lee, *J. Polymer Sci., Part A: Polym. Chem.*, 2004, **42**, 933-940.
17. J. Min, P. N. Shah, J.-H. Ahn and J.-S. Lee, *Macromolecules*, 2011, **44**, 3211-3216.
18. J.-H. Ahn, Y.-D. Shin, G. Y. Nath, S.-Y. Park, M. S. Rahman, S. Samal and J.-S. Lee, *J. Am. Chem. Soc.*, 2005, **127**, 4132-4133.
19. M. S. Rahman, H.-S. Yoo, M. Changez and J.-S. Lee, *Macromolecules*, 2009, **42**, 3927-3932.
20. P. N. Shah, J. Min and J.-S. Lee, *Chem. Commun.*, 2012, **48**, 826-828.
21. K. W. Henderson, D. S. Walther and P. G. Williard, *J. Am. Chem. Soc.*, 1995, **117**, 8680-8681.
22. A. V. Yakimansky and A. H. E. Müller, *Macromolecules*, 1999, **32**, 1731-1736.
23. A. V. Yakimansky and M. Van Beylen, *Polymer*, 2002, **43**, 5797-5805.
24. A. D. Becke, *Phys. Rev. A*, 1988, **38**, 3098-3100.

25. C. Lee, W. Yang and R. G. Parr, *Phys. Rev. B*, 1988, **37**, 785-789.
26. J. C. Slater, *Quantum Theory of Molecules and Solids. Vol. 4. The Self-Consistent Field for Molecules and Solids*, McGraw-Hill, New York, 1974.
27. S. H. Vosko, L. Wilk and M. Nusair, *Can. J. Phys.*, 1980, **58**, 1200-1211.
28. B. Miehlich, A. Savin, H. Stoll and H. Preuss, *Chem. Phys. Lett.*, 1989, **157**, 200-206.
29. *Jaguar 6.5 User Manual*, 2005, Schrodinger Inc., Portland, OR.
30. B. H. Greeley, T. V. Russo, D. T. Mainz, R. A. Friesner, J.-M. Langlois, W. A. Goddard III, R. E. Donnelly Jr. and M. N. Ringalda, *J. Chem. Phys.*, 1994, **101**, 4028-4041.
31. J. Geier, H. Rüegger and H. Grützmacher, *Dalton Trans.*, 2006, 129-136.
32. M. Rajeswaran, W. J. Begley, L. P. Olson and S. Huo, *Polyhedron*, 2007, **26**, 3653-3660.
33. D. R. Armstrong, W. Clegg, S. M. Hodgson, R. Snaith and A. E. H. Wheatley, *J. Organometal. Chem.*, 1998, **550**, 233-240.
34. D. R. Armstrong, R. P. Davies, P. R. Raithby, R. Snaith and A. E. H. Wheatley, *New J. Chem.*, 1999, **23**, 499-507.
35. H. Weiss, A. V. Yakimansky and A. H. E. Müller, *J. Am. Chem. Soc.*, 1996, **118**, 8897-8903.
36. G. Chang, W. C. Guida and W. C. Still, *J. Am. Chem. Soc.*, 1989, **111**, 4379-4386.
37. W. L. Jorgensen, D. S. Maxwell and J. Tirado-Rives, *J. Am. Chem. Soc.*, 1996, **118**, 11225-11236.
38. G. A. Kaminski, R. A. Friesner, J. Tirado-Rives and W. L. Jorgensen, *J. Phys. Chem. B*, 2001, **105**, 6474-6487.
39. *MacroModel 9.1 User Manual*, 2005, Schrodinger, LLC, New York, NY.
40. M. Mammen, E. I. Shakhnovich, J. M. Deutch and G. M. Whitesides, *J. Org. Chem.*, 1998, **63**, 3821-3830.
41. A. Yakimansky, G. Wang, K. Janssens and M. Van Beylen, *Polymer*, 2003, **44**, 6457-6463.
42. A. V. Yakimansky and A. H. E. Müller, *Macromolecules*, 2006, **39**, 4228-4234.
43. D. A. McQuarrie, *Statistical Mechanics*, University Science Books, Sausalito, 2000.
44. D. J. Tannor, B. Marten, R. Murphy, R. A. Friesner, D. Sitkoff, A. Nicholls, M. Ringnalda, W. A. Goddard, III and B. Honig, *J. Am. Chem. Soc.*, 1994, **116**, 11875-11882.
45. B. Marten, K. Kim, C. Cortis, R. A. Friesner, R. B. Murphy, M. N. Ringnalda, D. Sitkoff and B. Honig, *J. Phys. Chem.*, 1996, **100**, 11775-11788.
46. Y. H. Jang, W. A. Goddard III, K. T. Noyes, L. C. Sowers, S. Hwang and D. S. Chung, *J. Phys. Chem. B*, 2003, **107**, 344-357.
47. Y. H. Jang, W. A. Goddard III, K. T. Noyes, L. C. Sowers, S. Hwang and D. S. Chung, *Chem. Res. Toxicol.*, 2002, **15**, 1023-1035.
48. Y. H. Jang and W. A. Goddard, III, *J. Phys. Chem. B*, 2006, **110**, 7660-7665.
49. Y. H. Jang, S. Hwang, S. B. Chang, J. Ku and D. S. Chung, *J. Phys. Chem. A*, 2009, **113**, 13036-13040.
50. D. R. Lide, *CRC Handbook of Chemistry and Physics, 87th Ed.*, CRC Press, Boca Raton, 2006-2007.
51. T. E. Patten and B. M. Novak, *J. Am. Chem. Soc.*, 1996, **118**, 1906-1916.
52. M. H. Chisholm and M. W. Extine, *J. Am. Chem. Soc.*, 1977, **99**, 792-802.
53. D. Baskaran and A. H. E. Müller, in *Controlled and living polymerization* eds. A. H. E. Müller and K. Matyjaszewski, Wiley-VCH, Weinheim, Editon edn., 2009.
54. K. Janssens, E. Loozen, A. Yakimansky and M. Van Beylen, *Polymer*, 2009, **70**, 5368-5373.
55. X.-Q. Zhang, R. A. van Santen and A. P. J. Jansen, *Phys. Chem. Chem. Phys.*, 2012, **14**, 11969-11973.
56. X.-Q. Zhang, T. T. Trinh, R. A. van Santen and A. P. J. Jansen, *J. Am. Chem. Soc.*, 2014, **133**, 6613-6625.

The origin of the living nature in the isocyanate polymerization by sodium benzanilide (Na^+BA^-) initiators is understood from the relative stabilities of the $(NaBA)_n$ clusters in the polymerization condition (THF solution at 175 K).